

Carpet-3 detection of a photon-like air shower with estimated primary energy above 100 TeV in a spatial and temporal coincidence with GRB 221009A

D. D. Dzhappuev,¹ I. M. Dzaparova,¹ T. A. Dzhatdoev,^{1,2} E. A. Gorbacheva,¹ I. S. Karpikov,¹
M. M. Khadzhiev,¹ N. F. Klimenko,¹ A. U. Kudzhaev,¹ A. N. Kurenya,¹ A. S. Lidvansky,¹
O. I. Mikhailova,¹ V. B. Petkov,¹ E. I. Podlesnyi,³ N. A. Pozdnukhov,^{1,*} V. S. Romanenko,¹
G. I. Rubtsov,¹ S. V. Troitsky,^{1,2} I. B. Unatlokov,¹ N. A. Vasiliev,² A. F. Yanin,¹ and K. V. Zhuravleva¹
(Carpet-3 Group)

¹*Institute for Nuclear Research of the Russian Academy of Sciences,
60th October Anniversary Prospect 7a, Moscow 117312, Russia*

²*Lomonosov Moscow State University, 1-2 Leninskie Gory, Moscow 119991, Russia*

³*Norwegian University for Science and Technology (NTNU), Institutt for fysikk, Trondheim, Norway*

The brightest cosmic gamma-ray burst (GRB) ever detected, GRB 221009A, was accompanied by photons of very high energies. These gamma rays may be used to test both the astrophysical models of the burst and our understanding of long-distance propagation of energetic photons, including potential new-physics effects. Here we present the observation of a photon-like air shower with the estimated primary energy of 300_{-38}^{+43} TeV, coincident (with the chance probability of $\sim 9 \cdot 10^{-3}$) with the GRB in its arrival direction and time. Making use of the upgraded Carpet-3 muon detector and new machine learning analysis, we estimate the probability that the primary was hadronic as $\sim 3 \cdot 10^{-4}$. This is the highest-energy event ever associated with any GRB.

I. INTRODUCTION

Gamma-ray bursts (GRBs) are intense pulses of soft γ and hard X-rays emitted by astrophysical sources (for reviews see e.g. Refs. [1–7]). Typical observed fluences of GRBs are 10^{-7} erg/cm² $\lesssim F \lesssim 10^{-4}$ erg/cm², emitted with the characteristic duration of 10^{-2} s $\lesssim T_{90} \lesssim 10^3$ s encompassing 90% of the total GRB counts. Two distinct classes of GRBs were identified [8, 9]: short-duration, $T_{90} < 2$ s, GRBs that usually arise in the mergers of compact objects (two neutron stars or a neutron star and a black hole) in binary systems, and long-duration GRBs from the core collapse of massive, $M > 15M_{\odot}$, stars.

The prompt GRB emission [10] is the initial pulse revealing a highly irregular time structure. It is usually followed by an afterglow [11] that, as a rule, has a smooth light curve extending up to several days. By far the most popular GRB emission scenario invokes the production of the prompt emission in the shock waves internal to the fireball (e.g. [12]; for a recent treatment see e.g. [13]), while the afterglow is believed to be produced in external shock waves (e.g. [14–16]). The afterglow emission covers a wide range of energies from radio to γ rays. The lower energy part of the afterglow emission (radio to X rays) is mostly due to synchrotron radiation of electrons accelerated in the external shock wave [14, 15, 17, 18] while the high-energy part (X rays to TeV γ rays) may occur due to inverse Compton scattering of the synchrotron photons on the same electrons [17, 19–21]. Very high energy (VHE, $E > 100$ GeV) γ rays were detected from the afterglows of several GRBs [22–26].

On October 9, 2022, the Neil Gehrels Swift Observatory [27] and the Fermi Gamma-ray Burst Monitor

(Fermi-GBM) [28] detected an exceptionally bright γ -ray burst GRB 221009A, sometimes referred to as the brightest of all time (BOAT) [29]. This long-duration GRB has been detected by numerous instruments in the optical, X-ray and γ -ray domains [30–39]. The redshift of GRB 221009A was determined as $z = 0.151$ [40–42].

More than 60000 γ rays in the energy range 200 GeV – 7 TeV were recorded with the Large High Altitude Air Shower Observatory (LHAASO) Water Cherenkov Detector Array (WCDA) during 3000 s after the Fermi-GBM trigger [43]. The detection of γ rays with energies $E > 10$ TeV from GRB 221009A, never observed previously from any other GRB, was reported in [44]. The LHAASO 1.3 km² Array (KM2A) registered [44] 142 very high energy photon-like events in the energy range (3–20) TeV during the time window (230–900) s after the trigger, while 16.7 were expected from the cosmic-ray background. Nine of them have energies $\gtrsim 10$ TeV in the baseline reconstruction. For each of them, the probability that it is caused by a background cosmic ray lays between 0.045 and 0.17.

The TeV γ -ray flux from GRB 221009A should be strongly attenuated through the production of electron-positron pairs on extragalactic background light (EBL) photons, $\gamma\gamma \rightarrow e^+e^-$ [45, 46]. The energy of an individual LHAASO event, ~ 18 TeV, first reported in [47], as well as our preliminary announcement [48] of an event with > 200 TeV energy, attracted much attention in this context, and numerous new-physics explanations have been discussed. These include mixing of photons with axion-like particles [e.g. 49–59], Lorentz-invariance violation [e.g. 60–63], and other exotic scenarios [e.g. 64–70]. However, analyses of published LHAASO results [43, 44] alone do not require unconventional physics [44, 71–73], though may slightly prefer nonzero axion-photon coupling or Lorentz-invariance violation [44].

* Corresponding author; email: nikita.pozdnukhov1@gmail.com

In the present paper, we discuss in detail the Carpet-2 photon-like event associated with GRB 221009A and briefly reported in the telegram [48]. Building upon Ref. [48], we leverage data from the newly commissioned large-area muon detector, Carpet-3, which was operational at the time of the event. Dedicated simulations are employed to determine the event's characteristics, including energy and primary particle type, and to assess the probability of a chance association. In Sec. II, we first discuss the experiment and the data set and give references to details of the standard Carpet-2 reconstruction procedure (Sec. II A), then present information about the particular event associated with the GRB in Sec. II B. Section III presents details of the dedicated analysis of the event, including Monte-Carlo simulations, determination of the primary energy (Sec. III A) and confronting the event with standard photon selection criteria based on the muon number (Sec. III B). A more advanced classification of the primary particle of the event, based on machine learning, is presented in Sec. III C, see also Appendix B. We proceed in Sec. III D with the estimate of the effective area of the installation and of the GRB fluence implied by this detection. Section IV summarizes our results and puts them in context of the other studies.

II. DATA

A. Installation and data set

Carpet-3 is a ground-based air shower array located at the Baksan Neutrino Observatory of the Institute for Nuclear Research of the Russian Academy of Sciences (Neutrino village, North Caucasus; geographical coordinates 43.273° North, 42.685° East, 1700 m above sea level). The facility includes the central rectangular Carpet array of 400 liquid-scintillator detectors (20×20), each of dimensions of 70×70×30 cm³, providing a continuous area of the array of 196 m² supplemented by 4 outer stations. In each detector, the energy release is measured with a logarithmic charge-to-digital converter (LQDC), with energy threshold of 8 vertical equivalent muons (VEM). The central Carpet array allows localizing the shower axis and reconstructing the number of relativistic particles N_e in the shower, based on the Nishimura-Kamata-Greisen (NKG) function.

Each of the four outer detector stations (ODS) has 18 detectors (3×6) similar to the ones used in the central Carpet array, all PMT anode signals from which are summed up. The summed signals from each station are passed to a constant fraction discriminator (CFD) with a threshold of 0.5 VEM, and then to a time-to-digital converter (TDC) to measure time delays between the ODS, which are used to determine the arrival direction of the shower (the zenith angle θ and the azimuthal angle ϕ).

The underground muon detector (MD) consists of two parallel tunnels, each of which includes 205 plastic scintillator detectors (5×41) with dimensions of

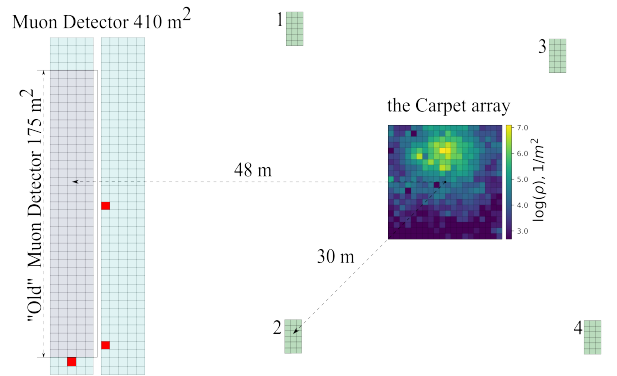


Figure 1. Layout (plot to scale) of the Carpet-3 EAS array and the display of the event associated with GRB 221009A. The central Carpet consists of 400 liquid-scintillator detectors (20×20) with a total area of 196 m². The color shows the relative energy release in each detector in a logarithmic scale. Outer detector stations (ODS) (light green) consist of 18 detectors (3×6) based on a liquid scintillator that are used to calculate the arrival direction of a shower. The underground muon detector (MD) includes 410 detectors (two tunnels with 5×41 in each) based on a plastic scintillator with a total area of 410 m², consisting of two parts: the old MD part 175 m² (grayish blue) and the new part 235 m² (light blue), used here for the first time for an astrophysical analysis. Detectors that triggered with a threshold greater than 0.5 VEM are highlighted in red.

100×100×5 cm³, providing the total MD area of 410 m². Historically, the muon detector was equipped with detectors in several stages. Initially, in the Carpet-2 experiment, its area was 175 m² and charge-digital converters (QDC) measured the total energy release in this area and estimated the total number n_{μ}^{175} of detected muons. In 2022, the modernization of MD for the Carpet-3 experiment was completed, as a result of which 235 detectors were added to the MD. Each of these detectors is equipped with a CFD, with a threshold of 0.5 VEM. Thus, the number n_{μ}^{235} of muons in the new MD is estimated based on the number of triggered detectors without measuring the energy release in them. The difference in the construction of the two parts of the MD is taken into account in the Monte Carlo simulations of the installation.

The layout of the installation collecting data at the day of GRB 221009A, as well as the display of the event we are discussing here, are presented in Fig. 1. For more detailed descriptions of the experiment, data, Monte-Carlo simulations and the standard analysis pipeline, see e.g. Refs. [74–79].

The standard extensive air shower (EAS) trigger for recording information about an event is formed by a coincidence circuit under the following condition:

- the total energy release in the central Carpet exceeds 15 VEM,

- four ODS's with a threshold of more than 0.5 VEM have triggered.

The typical frequency of this trigger is about 1.3 Hz.

We apply the following criteria when reconstructing events:

- the reconstructed shower axis is inside the central Carpet array excluding the detectors located at the boundary of the central array,
- the reconstructed energy release in the central Carpet array exceeds 5000 VEM,
- the number of triggered detectors of the central Carpet array exceeds 200,
- the reconstructed zenith angle $\theta \leq 40^\circ$.

All events that satisfy these criteria are included in the data set. The Carpet-3 data set we use here includes 108468 events with data from the 410 m² muon detector recorded between May 20, 2022 and December 31, 2024. Due to occasional maintenance, data collection was interrupted a few times. We include only full days of data collection in the analysis, and the number of these days is 667. In Appendix A, we discuss, for completeness, the 175 m² MD data which provide for a worse gamma-hadron separation but a much longer exposure.

B. The event associated with GRB 221009A

On October 9, 2022, at 14:32:35 UT, that is 1338 s after the Swift trigger and 4536 s after the Fermi-GBM trigger for GRB 221009A, the installation recorded an event with the reconstructed arrival direction $\alpha = 289.5^\circ$, $\delta = 18.4^\circ$ in equatorial (J2000) coordinates. This direction is 1.8° away from the GRB position in the sky, that is well within the Carpet-3 directional uncertainty (4.7° at the 90% CL). The reconstructed number N_e of relativistic particles for this shower is $N_e^{\text{ev}} = 36400$. This event had a zero response in the 175 m² muon detector, $n_\mu^{175, \text{ev}} = 0$, which indicated a rare photon-like event and invited us to publish the telegram [48]. Here, we present a dedicated study of this event using the full 410 m² detector data. The full MD registered $n_\mu^{\text{ev}} = 3$ muons. We will see below in Sec. III B that this is much lower than the typical n_μ of a shower with $N_e \sim N_e^{\text{ev}}$ and indicates a likely gamma-ray origin of the event. The readings of individual detector segments are shown in Fig. 1. For convenience, the basic information about the event is collected in Table I.

Before proceeding with a detailed analysis, we briefly estimate the probability that a background event coincided with the GRB by chance. The main background for gamma-ray detection with air-shower experiments comes from cosmic-ray events, which can occasionally be muon-poor due to fluctuations. However, the event of interest arrived from the direction close to the Galactic plane,

date	09.10.2022
time (UT)	14:32:35
$T - T_0$	4536 s
zenith angle	26.5°
right ascension	289.5°
declination	$+18.4^\circ$
distance from GRB	1.8°
N_e	36400
energy	300_{-38}^{+43} TeV
n_μ^{175}	0
n_μ	3
coincidence probability	$9.0 \cdot 10^{-3}$
primary hadron probability	$3 \cdot 10^{-4}$

Table I. Properties of the Carpet-3 event associated with GRB 221009A. See the text for details.

having the Galactic latitude $b \approx 4^\circ$. Galactic sources have been identified as emitters of gamma rays with energies above 100 TeV [80–82]; in particular, the unidentified source 3HWC J1928+178, possibly associated with LHAASO J1929+1745, is located in 2.5° from the best-fit arrival direction of the Carpet-3 event [83]. In addition, the diffuse Galactic-plane gamma-ray emission above 100 TeV has been detected [84, 85]. Though the sensitivity of present Carpet-3 analyses is insufficient to detect this source, nor to observe the Galactic-plane diffuse flux, occasional Galactic photons may contribute to the background for the GRB observation. The fluxes and spectra of the sources, and of the diffuse background in a given direction, are however known with large uncertainties, which preclude one from using them to model the background. Therefore, we choose to use a conservative data-driven estimate of the background, based on the actual rate of high-energy photon candidate events from the direction in the sky consistent with the GRB up to the Carpet-3 pointing accuracy.

Due to the Earth's rotation, a given direction in the sky is within the installation field of view for a certain period of time every day, under continuously changing zenith angle. One day is therefore a natural unit of observational time. We determine a high-energy photon-like event as one with reconstructed $N_e \geq N_e^{\text{ev}}$ and $n_\mu \leq n_\mu^{\text{ev}}$. In 667 live days in the data set, 2 such photon-like events (including the event associated with GRB 221009A) were detected from the circular area in the sky centered at the GRB direction in equatorial coordinates and having angular radius of Carpet-3 90% CL angular resolution. The Poisson probability of registration of an event satisfying these criteria on the day of GRB 221009A is $3.0 \cdot 10^{-3}$, and it does not require trial corrections. Note that the pre-trial p-value of 1.2×10^{-4} reported in the Carpet-2 telegram [48] was obtained in a similar way but (i) using the time interval of 4536 s instead of one day, (ii) with slightly stricter criteria for selection of high-energy photon candidates, and (iii) without the 410 m² MD infor-

mation.

It is important to note that, by construction, the data-driven background, used for the estimate of the probability of a chance coincidence, includes all muon-poor events, no matter if they were caused by unusual cosmic rays or by gamma rays from other sources.

III. ANALYSIS

A. Monte-Carlo simulations and the primary energy

Reconstruction of the properties of the primary particle requires Monte-Carlo (MC) simulations. The standard Carpet-2 MC procedure was described in [86]. The response of the detector to artificial showers is modeled with a dedicated code and stored in the same format as the experimental data are stored. The reconstruction of the MC events is performed by the same procedure and codes for both real and simulated data.

To analyze the event of interest in more detail, we have generated 6750 air showers caused by primary photons and 6750 showers caused by protons with energies between 100 TeV and 1000 TeV. We use the CORSIKA 7.7420 [87] EAS simulation package with QGSJET-II-04 [88] as the high-energy hadronic interaction model and FLUKA2011.2c [89] as the low-energy hadronic interaction model. All showers are modeled in the energy range 100-1000 TeV with a spectrum $dN/dE_0 \propto E_0^{-2}$. The arrival directions of the simulated primary particles are sampled from a two-dimensional Gaussian distribution centered at the initially reconstructed arrival direction of the event of interest, with the dispersion reproducing the 90% CL containment angle of 4.7° . The full Monte-Carlo set contains 80609 events.

To estimate the energy of an event associated with GRB 221009A, we use the dependence of N_e on the primary energy obtained by fitting the results of the MC simulations for the gamma-ray primaries to a power law. This results in the estimate $E_\gamma^{\text{ev}} = 300_{-38}^{+43}$ TeV assuming that the event was caused by a photon. The full MC simulation data, including the proton primaries, is used in Sec. III C.

B. Muon number

We have pointed out that the event associated with the GRB is unusual in terms of its low muon number. We quantify this statement in this section by comparing the observed event with typical air showers of that size detected by Carpet-3 and with simulated gamma-ray induced showers in terms of n_μ .

The expected distribution of n_μ for bulk air showers consistent with the GRB-associated event in energy and zenith angle is obtained as follows. We weight the events

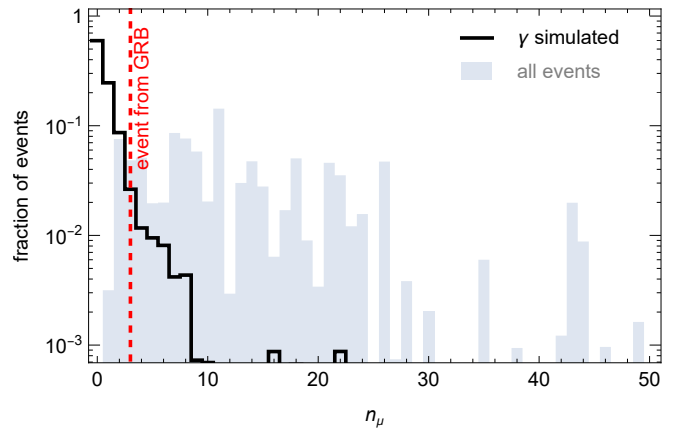


Figure 2. Distribution (PDF) of the number of muons in the Carpet-3 MD. The shaded histogram represents the data; the black histogram represents the simulations assuming gamma-ray primaries; the value $n_\mu = 3$ of the GRB-associated event is shown by the vertical dashed line. Event contributions are weighted, as discussed in the text. Note the log scale of the vertical axis.

in real data according to their reconstructed N_e and arrival direction in the horizontal coordinates, azimuth and zenith angles. The weight is calculated as a product of log-normal distribution in N_e , centered at N_e^{ev} and having the width corresponding to the $\pm 15\%$ statistical error in N_e , and of the two-dimensional Gaussian distribution of directions centered in the observed direction and reproducing the 90% CL angular resolution of 4.7° . In the simulation data, the angles of arrival are modeled already taking into account the two-dimensional Gaussian distribution. The model events are weighted taking into account the log-normal distribution of N_e , similar to the real data.

The obtained distributions are shown in Fig. 2). The fraction of hadronic events that are expected to have $n_\mu \leq 3$ in the 410 m² MD is 0.127. While the observed event is indeed more photon-like than most of detected EAS, we see that it is not that rare, when the information from the full 410 m² MD is considered (see Appendix A for the 175 m² case). In the following Sec. III C, we add more observational information and use a more advanced method to test the photonic origin of the observed event.

C. Neural network gamma-ray classification

We estimate the type of primary particle using a neural network classifier trained on the MC event set described above in Sec. III A. The network is trained to distinguish between events with proton and photon primary particles. The signals from 400 scintillator detectors of the central Carpet array are used as a classifier input along with some of the reconstructed parameters, namely, the arrival direction (θ, ϕ) , the shower axis coordinates at the ground level, N_e , the number of muons in the 175 m²

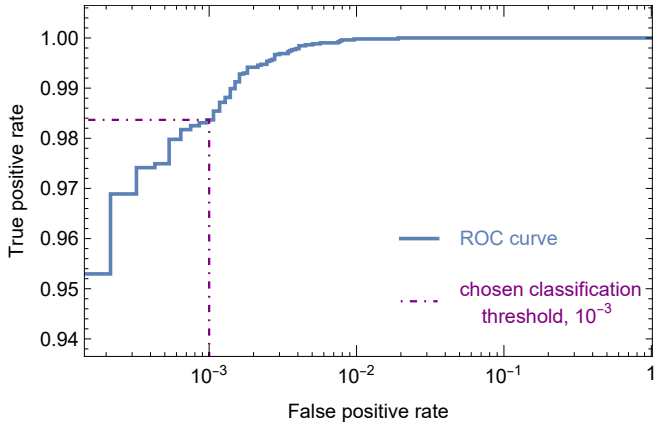


Figure 3. ROC curve of the gamma-ray – proton classifying neural network, evaluated on the test set. The chosen threshold is shown as a dot-dashed line.

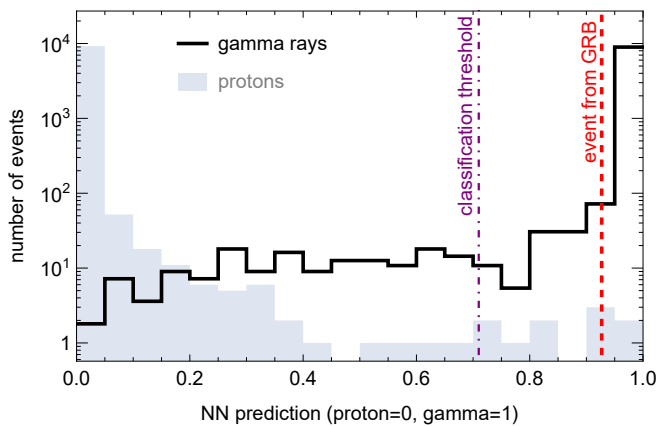


Figure 4. Predictions distribution of the gamma-ray – proton classifying neural network. The values of the classification threshold (0.71; dot-dashed line) and of the prediction for the event analyzed in this work (0.927; dashed line) are shown.

detector, the number of muons in the 410 m² detector, and the variable C_k introduced in [90] that measures the azimuthal nonuniformity of the shower at the ground level. The network itself consists of a convolutional part handling the spatial detector data, which is essentially a 20-by-20 pixel image, and a fully-connected part for the reconstructed parameters. The full architecture of the neural-network classifier is presented in Appendix B.

The Monte Carlo set is split into training and test sets, which consist of 62007 and 18602 events, correspondingly. The test set is used for evaluation of the network after training. Fig. 3 shows the resulting receiver operating characteristic (ROC) curve. It demonstrates that the network performs well on the MC data, reaching 10^{-3} proton background rejection factor without a significant decrease in the photon selection efficiency. Fig. 4 presents the network prediction distribution. A prediction of 1 corresponds to a photon event, 0 to a proton event. For a chosen background rejection factor of 10^{-3} , the clas-

sification threshold is equal to 0.71. This means that events with prediction values above 0.71 are classified as photons.

We then use the classifier for the event discussed in this work. Data are processed and normalized in the same way as in MC simulations. The resulting prediction value is 0.927, well above the classifier threshold. This gives additional evidence for the photon nature of this event. Based on simulations, the probability that this event is a misclassified hadron is $\approx 3 \cdot 10^{-4}$. This is calculated as the fraction of MC hadrons that the network incorrectly classifies as photons with the same or higher prediction values.

Within the angular resolution of Carpet-3 of 4.7 degrees, there were 6 events in 667 live days of data having $N_e \geq N_e^{\text{ev}}$ and the same or higher value of neural network prediction, that is, more photon-like, than the GRB-associated event. The probability that a background high-energy photon-like event could arrive on the day of the gamma-ray burst is therefore $9.0 \cdot 10^{-3}$.

D. Effective area and fluence estimates

For a fast transient like a GRB, it is not straightforward to compare fluxes measured by different instruments in non-coinciding period of time. A useful quantity to compare is fluence, that is the amount of energy per unit area integrated over the entire time of the burst. To estimate the fluence, one needs some assumptions about the source, in particular, about its spectrum, which we assume here to be a E^{-2} power law. This spectrum is then convolved with the energy-dependent effective area of the installation to obtain the total number of events expected to be detected. Equating this number to the observed one, we obtain the normalization of the assumed spectrum and estimate the fluence.

The effective area of Carpet-3 is determined by a product of the geometrical area of the installation and the efficiency for photon detection, estimated from Monte-Carlo simulations. For the selection cuts used here, which imply reconstructed shower axes within the central Carpet but without the perimeter detector stations, the geometrical area is 1.6×10^6 cm². The efficiency depends on both primary energy E_γ and zenith angle θ . To estimate it, we have thrown Monte-Carlo air showers with gamma-ray primaries to the area considerably larger than the installation and find a ratio between the number of events passed all selection criteria and the number of thrown showers with axes within the geometrical area we use. The dependence of efficiency on E_γ and θ is shown in Fig. 5. For parameters of the event associated with GRB 221009A, the efficiency is 0.38. Note that this simulation assumed the selection criteria used in the present work, so the values of efficiency plotted in Fig. 5 may not be applicable to other analyses.

The estimated GRB 221009A fluence above 100 TeV is $\mathcal{F} \approx (1.1 \pm 0.9) \times 10^{-3}$ erg/cm² (68% CL), which is in a

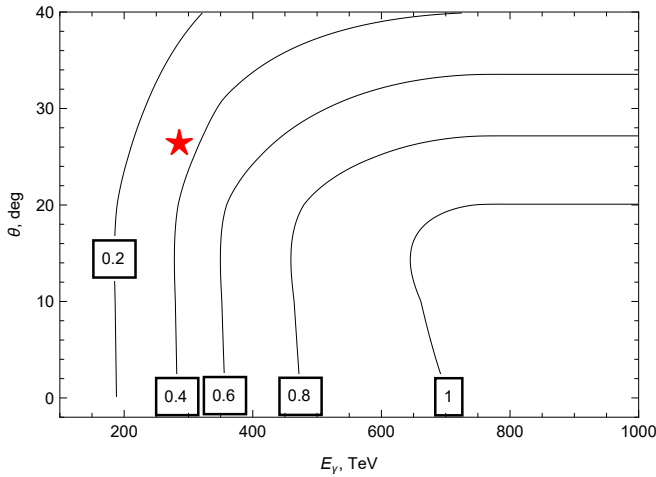


Figure 5. Contour plot of the photon detection efficiency as a function of energy and zenith angle for the selection cuts adopted in the present work. Numbers in squares represent the efficiency values. The star indicates the values for the GRB-associated event.

reasonable agreement with the values found in the lower energy bands, corrected for absorption. The estimate is based on a single event and thus suffers from large uncertainties, estimated here based on the Poisson statistics as recommended by Ref. [91].

IV. DISCUSSION AND CONCLUSIONS

A. Observational conditions

We report on the Carpet-3 observation of a rare photon-like air shower, whose arrival direction and time match those of the exceptional GRB 221009A. Other experiments, including larger ones, have not reported events with those high energies from this, nor from any other, GRB. This may be related to the temporal structure of the very high energy afterglow, combined with visibility conditions for different experiments. Indeed, Carpet-3 observed the event 4536 s after the burst trigger, high above the horizon (see Fig. 6). At this moment, the burst site was seen at considerably larger zenith angle at LHAASO, close to the limit of the field of view of the experiment. LHAASO did not report on the GRB 221009A observations beyond 2000 s post trigger. For High-Altitude Water Cerenkov Detector (HAWC), the direction of interest was below the horizon [92].

LHAASO observed a hardening of the gamma-ray spectrum with time for GRB 221009A [43, 44]. Very high energy, $E > 100$ GeV, photons have been detected even days after the trigger both from GRB 221009A by Fermi Large Area Telescope (LAT) [93–95] and from GRB 190829A by the High Energy Stereoscopic System (H.E.S.S.) [96]. A quantitative assessment of the development of the afterglow at high energies would be strongly

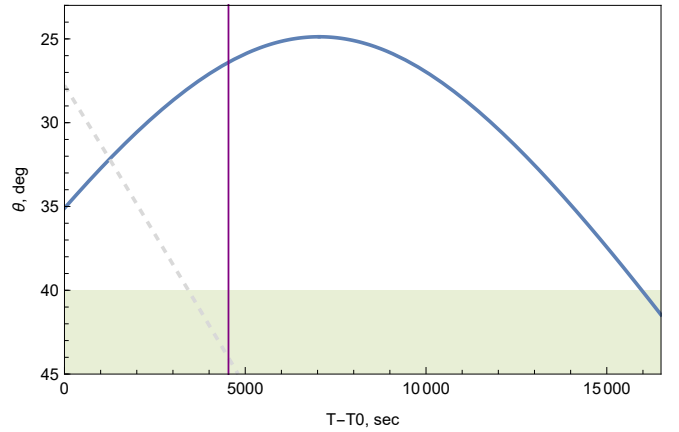


Figure 6. Temporal dependence of the zenith angle of the GRB 221009A as seen by Carpet-3 (full blue line). The dashed gray line is the same dependence for LHAASO. The vertical maroon line indicates the Carpet-3 event arrival time. The shaded area at the bottom corresponds to zenith angles $\theta > 40^\circ$ excluded in the analysis.

model-dependent.

B. Origin of energetic photons in GRB

Let us discuss briefly several possible mechanisms of multi-TeV gamma-ray production in the afterglow of GRB 221009A. Below the observable gamma-ray energy of several TeV, the most natural mechanism of gamma-ray production in GRB afterglows is synchrotron self-Compton (SSC) [23, 97]. Above the observed energy of 10 TeV, however, the Klein-Nishina effect typically sets in, resulting in a significant suppression of the interaction rate between the electrons and photons, leading to a downturn in the produced gamma-ray spectrum. Therefore, another mechanism is needed to produce the observable γ -rays with the energy $E > 100$ TeV.

It is hardly possible to explain the detection of the reported event with the proton synchrotron radiation. Indeed, the maximum characteristic energy of the synchrotron photons produced by the accelerating protons is $E_{\text{sp,max}} \sim 100$ GeV (in the plasma comoving rest frame) [98]. The maximum observable energy of the same photons is $E_{\text{sp,max}} \times D / (1 + z) \sim 1$ TeV since the value of the Doppler factor D could hardly significantly exceed ten at relatively late time, thousands of seconds after the trigger. We note that the synchrotron-photon energy upper limit of [98] does not apply for secondary charged particles, e.g. for electrons and positrons produced in photohadronic or hadronuclear interactions.

Likewise, the photohadronic scenario for the event is strongly disfavoured due to the very low efficiency of the photopion process. As it is commonly done for blazars (for instance, see Ref. [99]), a very strong upper bound on the efficiency could be set from the apparent absence of strong absorption of GeV-TeV gamma rays in the ob-

servable spectrum of GRB 221009A.

Therefore, a nonconventional astrophysical mechanism is required to produce delayed, $\gtrsim 500$ s, gamma rays with the energy of ~ 10 TeV or higher. One such example was presented in [100], inspired by previous studies that accounted for interactions of high-energy neutrons escaping from their sources [101–106]. During the GRB prompt emission phase, protons and/or nuclei could be accelerated to high energies, $E > 1$ PeV/nucleon in the fireball rest frame. In contrast to the later afterglow phase (> 2000 s after the Fermi-GBM trigger), during the prompt emission phase the accelerated protons and/or nuclei interact with the dense photon fields inside the fireball relatively efficiently, producing gamma rays, electrons, positrons, neutrinos, and neutrons¹. These neutrons escape from the magnetic fields of the fireball freely and then interact with the interstellar matter of the star-forming region (SFR) where the GRB is located, creating a flux of hyper-relativistic electrons and positrons. These, in turn, radiate synchrotron photons in the magnetic field of the SFR, eventually producing an observable flux of gamma rays at energies $E \sim 10$ TeV for typical values of parameters. For an order-of-magnitude stronger than typical SFR magnetic field, or ≈ 3 -4 times higher energy of the accelerated protons, the observable gamma-ray energy of ~ 100 TeV is achievable in this scenario. The time delay comes from the angular spread of the neutron beam [106]. Thus, the proposed mechanism assumes the presence of a delayed “echo” from the prompt emission induced by the escaping and interacting energetic neutrons.

C. Comparison with the LHAASO fluence

In Ref. [44], LHAASO presented the observed energy spectra, based on the combination of WCDA and KM2A data, and the best power-law fits of the spectrum corrected for absorption within the extragalactic background light model of Ref. [109]. The spectra have been presented for two intervals, 230 s to 300 s and 300 s to 900 s after the trigger. It has also been demonstrated there that the light curve presented in Ref. [43] for WCDA fits well the KM2A observations up to the highest energies, thus the energy emitted between 900 s and 2000 s can be estimated. We use this information to obtain the differential fluence, $d\mathcal{F}/dE$, as the function of energy E , from the LHAASO measurements. The same quantity, estimated at the energy of the Carpet-3 observed events from the result of Sec. III D, is in order-of-magnitude agreement with the extrapolation of the *intrinsic* spectrum determined by LHAASO, see Fig. 7.

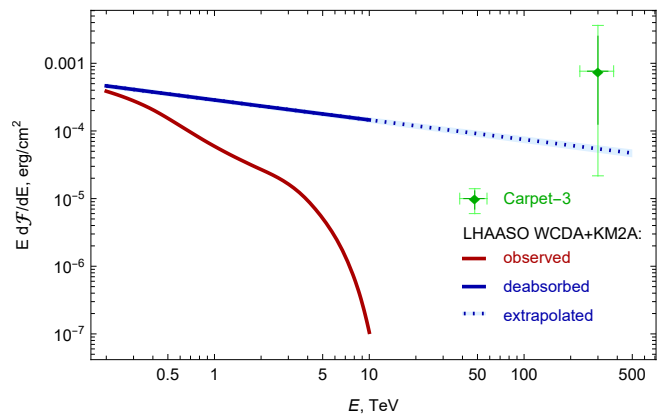


Figure 7. Comparison of the photon fluence of GRB 221009A estimated from the Carpet-3 observation (dark green: 68% CL, light green: 95% CL errors) with the extrapolation of LHAASO results.

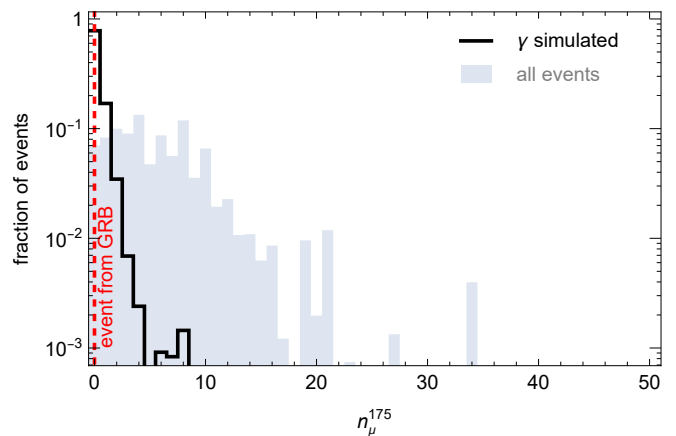


Figure 8. Same as Fig. 2 but for the 175 m² Carpet-2 MD.

D. Conclusions

As we discussed above, gamma rays with the energies of ~ 300 TeV cannot reach us from extragalactic sources, provided the Standard Model of particle physics describes correctly the photon propagation. Therefore, if the event reported here is a photon (we estimate the probability of the gamma-ray primary as $1 - 3 \cdot 10^{-4} = 0.9997$) arrived from GRB 221009A (probability $1 - 9 \cdot 10^{-3} = 0.991$), and reached us from the GRB site, then its detection by Carpet-3 could be seen as a manifestation of new fundamental physics. Relevant scenarios have been explored in the literature discussed in Sec. I and will be scrutinized, with the help of the information about the Carpet-3 event presented here, in future publications. The presented results are also relevant for constraining the strength of extragalactic magnetic fields, and for understanding the mechanisms of GRB emission at very high energies.

¹ Specific parameters of this scenario may be constrained from non-observation of high-energy neutrinos from GRB 221009A by IceCube [107] and KM3NeT [108].

ACKNOWLEDGEMENTS

We are indebted to L. Bezrukov, N. Kalmykov, P. Satunin and Yu. Stenkin for interesting discussions. This work is supported in the framework of the State project “Science” by the Ministry of Science and Higher Education of the Russian Federation under the contract 075-15-2024-541.

DATA AVAILABILITY

The data used in this study are available from the corresponding author upon a reasonable request.

Appendix A: Carpet–2: the 175 m² muon detector

The Carpet–2 data set of April 7, 2018 - December 31, 2024 includes 261468 events detected with the 175 m² MD data in 1676 live days. The number of events with $N_e > N_e^{ev}$ and $n_\mu = 0 = n_\mu^{175}$, within 4.7° from the GRB 221009A direction, is 7, including the event under study. The probability of registering an event that satisfies these criteria on the day of GRB 221009A is $4.2 \cdot 10^{-3}$. For completeness, we also provide a conservative estimate that the discussed event may be caused by a hadronic primary using only the old 175 m² MD data, see Fig. 8, as 0.070. We do not perform the machine-learning analysis for Carpet–2 data here because of lower photon-hadron separation power of the old MD.

Appendix B: The architecture of the neural network

Fig. 9 shows the architecture of the neural network classifier used in the present paper. The central Carpet array can be seen as a 20-by-20 pixel image, which is submitted as the input to a convolutional part of the network. The sizes of the filters are chosen to be sensitive to typical sub-clusters in the spatial data. Then, the output of this part is merged with the reconstructed data and fed forward to several fully connected layers.

The number and size of those layers are chosen based on the performance on the training data. The reconstructed parameters used are arrival angles θ and ϕ , shower axis coordinates at ground level X, Y , the number of muons n_μ^{175} in the old 175m² muon detector part, the number of muons n_μ^{410} in the full 410m² muon detector, shower size N_e and the variable C_k , introduced in [90].

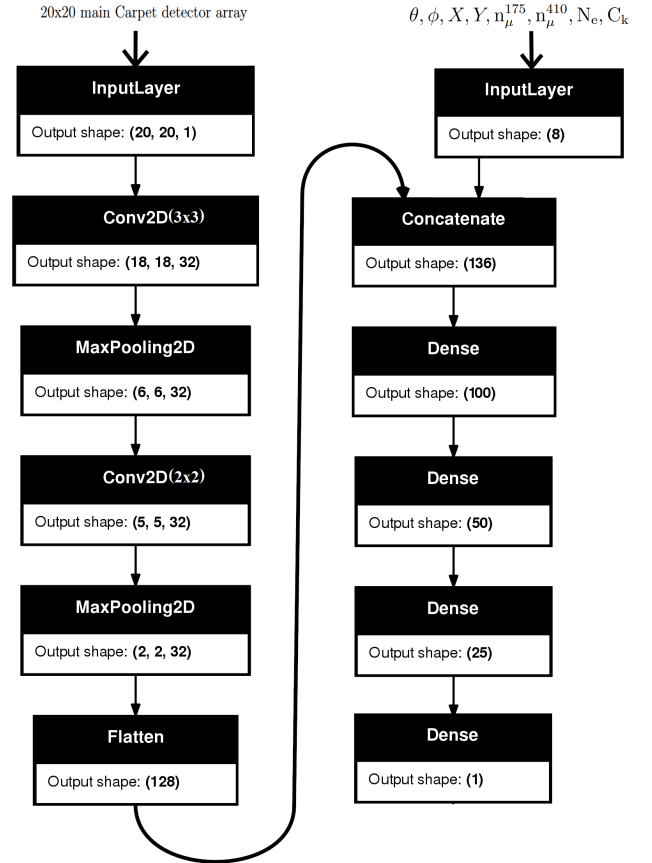


Figure 9. The architecture of the neural network classifier. *Keras* [110] and *Tensorflow* [111] are used as an application programming interface (API) for the neural network.

-
- [1] G. J. Fishman and C. A. Meegan, Gamma-ray bursts, *Ann. Rev. Astron. Astrophys.* **33**, 415 (1995).
 - [2] T. Piran, Gamma-ray bursts and the fireball model, *Phys. Rept.* **314**, 575 (1999), arXiv:astro-ph/9810256.
 - [3] T. Piran, Gamma-ray bursts: A puzzle being resolved, *Phys. Rept.* **333**, 529 (2000), arXiv:astro-ph/9907392.
 - [4] T. Piran, The physics of gamma-ray bursts, *Rev. Mod. Phys.* **76**, 1143 (2004), arXiv:astro-ph/0405503.
 - [5] P. Meszaros, Gamma-Ray Bursts, *Rept. Prog. Phys.* **69**, 2259 (2006), arXiv:astro-ph/0605208.
 - [6] P. Kumar and B. Zhang, The physics of gamma-ray bursts & relativistic jets, *Phys. Rept.* **561**, 1 (2015), arXiv:1410.0679 [astro-ph.HE].
 - [7] Z. Dai, F. Daigne, and P. Mészáros, The Theory of Gamma-Ray Bursts, *Space Sci. Rev.* **212**, 409 (2017).
 - [8] C. Kouveliotou, C. A. Meegan, G. J. Fishman, N. P. Bhyat, M. S. Briggs, T. M. Koshut, W. S. Paciesas, and G. N. Pendleton, Identification of two classes of gamma-ray bursts, *Astrophys. J. Lett.* **413**, L101 (1993).
 - [9] G. Ghirlanda, L. Nava, G. Ghisellini, A. Celotti, and C. Firmani, Short versus Long Gamma-Ray Bursts:

- spectra, energetics, and luminosities, *Astron. Astrophys.* **496**, 585 (2009), arXiv:0902.0983 [astro-ph.HE].
- [10] R. W. Klebesadel, I. B. Strong, and R. A. Olson, Observations of Gamma-Ray Bursts of Cosmic Origin, *Astrophys. J. Lett.* **182**, L85 (1973).
- [11] E. Costa *et al.*, Discovery of an X-ray afterglow associated with the gamma-ray burst of 28 February 1997, *Nature* **387**, 783 (1997), arXiv:astro-ph/9706065.
- [12] M. J. Rees and P. Meszaros, Unsteady outflow models for cosmological gamma-ray bursts, *Astrophys. J. Lett.* **430**, L93 (1994), arXiv:astro-ph/9404038.
- [13] S. k. M. Rahaman, J. Granot, and P. Beniamini, Prompt gamma-ray burst emission from internal shocks – new insights, *Mon. Not. Roy. Astron. Soc.* **528**, L45 (2023), arXiv:2308.00403 [astro-ph.HE].
- [14] M. J. Rees and P. Mészáros, Relativistic fireballs: energy conversion and time-scales, *Mon. Not. Roy. Astron. Soc.* **258**, 41P (1992).
- [15] P. Meszaros and M. J. Rees, Optical and long wavelength afterglow from gamma-ray bursts, *Astrophys. J.* **476**, 232 (1997), arXiv:astro-ph/9606043.
- [16] R. Sari, T. Piran, and R. Narayan, Spectra and light curves of gamma-ray burst afterglows, *Astrophys. J. Lett.* **497**, L17 (1998), arXiv:astro-ph/9712005.
- [17] P. Meszaros, P. Laguna, and M. J. Rees, Gas dynamics of relativistically expanding gamma-ray burst sources: Kinematics, energetics, magnetic fields and efficiency, *Astrophys. J.* **415**, 181 (1993), arXiv:astro-ph/9301007.
- [18] B. Paczynski and J. E. Rhoads, Radio transients from gamma-ray bursters, *Astrophys. J. Lett.* **418**, L5 (1993), arXiv:astro-ph/9307024.
- [19] P. Meszaros and M. J. Rees, Delayed GeV emission from cosmological gamma-ray bursts: Impact of a relativistic wind on external matter, *Mon. Not. Roy. Astron. Soc.* **269**, L41 (1994), arXiv:astro-ph/9404056.
- [20] P. Meszaros, M. J. Rees, and H. Papathanassiou, Spectral properties of blast wave models of gamma-ray burst sources, *Astrophys. J.* **432**, 181 (1994), arXiv:astro-ph/9311071.
- [21] R. Sari and A. A. Esin, On the Synchrotron self-compton emission from relativistic shocks and its implications for gamma-ray burst afterglows, *Astrophys. J.* **548**, 787 (2001), arXiv:astro-ph/0005253.
- [22] V. A. Acciari *et al.* (MAGIC), Teraelectronvolt emission from the γ -ray burst GRB 190114C, *Nature* **575**, 455 (2019), arXiv:2006.07249 [astro-ph.HE].
- [23] V. A. Acciari *et al.* (MAGIC), Observation of inverse Compton emission from a long γ -ray burst, *Nature* **575**, 459 (2019), arXiv:2006.07251 [astro-ph.HE].
- [24] H. Abdalla *et al.*, A very-high-energy component deep in the γ -ray burst afterglow, *Nature* **575**, 464 (2019), arXiv:1911.08961 [astro-ph.HE].
- [25] H. Abdalla *et al.* (H.E.S.S.), Revealing x-ray and gamma ray temporal and spectral similarities in the GRB 190829A afterglow, *Science* **372**, 1081 (2021), arXiv:2106.02510 [astro-ph.HE].
- [26] O. Blanch *et al.*, GRB 201216C: MAGIC detection in very high energy gamma rays, *GRB Coordinates Network* **29075**, 1 (2020).
- [27] M. A. Williams *et al.*, GRB 221009A: Discovery of an Exceptionally Rare Nearby and Energetic Gamma-Ray Burst, *Astrophys. J. Lett.* **946**, L24 (2023), arXiv:2302.03642 [astro-ph.HE].
- [28] S. Lesage *et al.*, Fermi-GBM Discovery of GRB 221009A: An Extraordinarily Bright GRB from Onset to Afterglow, *Astrophys. J. Lett.* **952**, L42 (2023), arXiv:2303.14172 [astro-ph.HE].
- [29] E. Burns *et al.*, GRB 221009A: The BOAT, *Astrophys. J. Lett.* **946**, L31 (2023), arXiv:2302.14037 [astro-ph.HE].
- [30] M. Negro *et al.*, The IXPE View of GRB 221009A, *Astrophys. J. Lett.* **946**, L21 (2023), arXiv:2301.01798 [astro-ph.HE].
- [31] M. D. Fulton *et al.*, The Optical Light Curve of GRB 221009A: The Afterglow and the Emerging Supernova, *Astrophys. J. Lett.* **946**, L22 (2023), arXiv:2301.11170 [astro-ph.HE].
- [32] D. A. Kann *et al.*, GRANDMA and HXMT Observations of GRB 221009A: The Standard Luminosity Afterglow of a Hyperluminous Gamma-Ray Burst—In Gedenken an David Alexander Kann, *Astrophys. J. Lett.* **948**, L12 (2023), arXiv:2302.06225 [astro-ph.HE].
- [33] T. Laskar *et al.*, The Radio to GeV Afterglow of GRB 221009A, *Astrophys. J. Lett.* **946**, L23 (2023), arXiv:2302.04388 [astro-ph.HE].
- [34] A. J. Levan *et al.*, The First JWST Spectrum of a GRB Afterglow: No Bright Supernova in Observations of the Brightest GRB of all Time, GRB 221009A, *Astrophys. J. Lett.* **946**, L28 (2023), arXiv:2302.07761 [astro-ph.HE].
- [35] J. Ripa *et al.*, The peak flux of GRB 221009A measured with GRBAlpha, *Astron. Astrophys.* **677**, L2 (2023), arXiv:2302.10047 [astro-ph.HE].
- [36] D. Frederiks *et al.*, Properties of the Extremely Energetic GRB 221009A from Konus-WIND and SRG/ART-XC Observations, *Astrophys. J. Lett.* **949**, L7 (2023), arXiv:2302.13383 [astro-ph.HE].
- [37] B. Stern and I. Tkachev, GRB 221009A, Its Precursor, and Two Afterglows in the Fermi Data, *JETP Lett.* **118**, 553 (2023), arXiv:2303.03855 [astro-ph.HE].
- [38] M. Tavani *et al.*, AGILE Gamma-Ray Detection of the Exceptional GRB 221009A, *Astrophys. J. Lett.* **956**, L23 (2023), arXiv:2309.10515 [astro-ph.HE].
- [39] C. Zheng *et al.*, Observation of GRB 221009A Early Afterglow in X-Ray/Gamma-Ray Energy Bands, *Astrophys. J. Lett.* **962**, L2 (2024), arXiv:2310.10522 [astro-ph.HE].
- [40] A. de Ugarte Postigo *et al.*, GRB 221009A: Redshift from X-shooter/VLT, *GRB Coordinates Network* **32648**, 1 (2022).
- [41] A. J. Castro-Tirado *et al.*, GRB 221009A: 10.4m GTC spectroscopic redshift confirmation, *GRB Coordinates Network* **32686**, 1 (2022).
- [42] D. B. Malesani *et al.*, The brightest GRB ever detected: GRB 221009A as a highly luminous event at $z = 0.151$ (2023), arXiv:2302.07891 [astro-ph.HE].
- [43] Z. Cao *et al.* (LHAASO), A tera-electron volt afterglow from a narrow jet in an extremely bright gamma-ray burst, *Science* **380**, adg9328 (2023), arXiv:2306.06372 [astro-ph.HE].
- [44] Z. Cao *et al.* (LHAASO), Very high energy gamma-ray emission beyond 10 TeV from GRB 221009A, *Sci. Adv.* **9**, adj2778 (2023), arXiv:2310.08845 [astro-ph.HE].
- [45] A. Nikishov, Absorption of high-energy photons in the universe, *Sov. Phys. JETP* **14**, 393 (1962), [*Zh. Eksp. Teor. Fiz.* **41** (1962) 549].

- [46] R. J. Gould and G. P. Schreder, Opacity of the Universe to High-Energy Photons, *Phys. Rev.* **155**, 1408 (1967).
- [47] Y. Huang *et al.*, LHAASO observed GRB 221009A with more than 5000 VHE photons up to around 18 TeV, GCN Circular **32677** (2022).
- [48] D. Dzhappuev *et al.*, Swift J1913.1+1946/GRB 221009A: detection of a 250-TeV photon-like air shower by Carpet-2, *The Astronomer's Telegram* **15669** (2022).
- [49] G. Galanti, L. Nava, M. Roncadelli, F. Tavecchio, and G. Bonnoli, Observability of the Very-High-Energy Emission from GRB 221009A, *Phys. Rev. Lett.* **131**, 251001 (2023), arXiv:2210.05659 [astro-ph.HE].
- [50] S. V. Troitsky, Parameters of axion-like particles required to explain high-energy photons from GRB 221009A, *Pisma Zh. Eksp. Teor. Fiz.* **116**, 745 (2022), arXiv:2210.09250 [astro-ph.HE].
- [51] A. Baktash, D. Horns, and M. Meyer, Interpretation of multi-TeV photons from GRB221009A, (2022), arXiv:2210.07172 [astro-ph.HE].
- [52] G. Galanti, M. Roncadelli, and F. Tavecchio, Assessment of ALP scenarios for GRB 221009A, (2022), arXiv:2211.06935 [astro-ph.HE].
- [53] W. Lin and T. T. Yanagida, Electroweak Axion in Light of GRB221009A, *Chin. Phys. Lett.* **40**, 069801 (2023), arXiv:2210.08841 [hep-ph].
- [54] S. Nakagawa, F. Takahashi, M. Yamada, and W. Yin, Axion dark matter from first-order phase transition, and very high energy photons from GRB 221009A, *Phys. Lett. B* **839**, 137824 (2023), arXiv:2210.10022 [hep-ph].
- [55] G. Zhang and B.-Q. Ma, Axion-Photon Conversion of LHAASO Multi-TeV and PeV Photons, *Chin. Phys. Lett.* **40**, 011401 (2023), arXiv:2210.13120 [hep-ph].
- [56] P. Carezza and M. C. D. Marsh, On ALP scenarios and GRB 221009A, (2022), arXiv:2211.02010 [astro-ph.HE].
- [57] L. Wang and B.-Q. Ma, Axion-photon conversion of GRB221009A, *Phys. Rev. D* **108**, 023002 (2023), arXiv:2304.01819 [astro-ph.HE].
- [58] D. A. Rojas, S. Hernández-Cadena, M. M. González, A. Pratts, R. Alfaro, and J. Serna-Franco, GRB 221009A: Spectral Signatures Based on ALPs Candidates, *Astrophys. J.* **966**, 114 (2024), arXiv:2305.05145 [astro-ph.HE].
- [59] S. Troitsky, Towards a model of photon-axion conversion in the host galaxy of GRB 221009A, *JCAP* **01**, 016, arXiv:2307.08313 [astro-ph.HE].
- [60] J. Zhu and B.-Q. Ma, Light speed variation from GRB 221009A, *J. Phys. G* **50**, 06LT01 (2023), arXiv:2210.11376 [astro-ph.HE].
- [61] J. D. Finke and S. Razzaque, Possible Evidence for Lorentz Invariance Violation in Gamma-Ray Burst 221009A, *Astrophys. J. Lett.* **942**, L21 (2023), arXiv:2210.11261 [astro-ph.HE].
- [62] H. Li and B.-Q. Ma, Lorentz invariance violation induced threshold anomaly versus very-high energy cosmic photon emission from GRB 221009A, *Astropart. Phys.* **148**, 102831 (2023), arXiv:2210.06338 [astro-ph.HE].
- [63] H. Li and B.-Q. Ma, Revisiting Lorentz invariance violation from GRB 221009A, *JCAP* **10**, 061, arXiv:2306.02962 [astro-ph.HE].
- [64] K. Cheung, The Role of a Heavy Neutrino in the Gamma-Ray Burst GRB-221009A, (2022), arXiv:2210.14178 [hep-ph].
- [65] A. Y. Smirnov and A. Trautner, GRB 221009A Gamma Rays from the Radiative Decay of Heavy Neutrinos?, *Phys. Rev. Lett.* **131**, 021002 (2023), arXiv:2211.00634 [hep-ph].
- [66] V. Brdar and Y.-Y. Li, Neutrino origin of LHAASO's 18 TeV GRB221009A photon, *Phys. Lett. B* **839**, 137763 (2023), arXiv:2211.02028 [hep-ph].
- [67] J. Huang, Y. Wang, B. Yu, and S. Zhou, Invisible neutrino decays as origin of TeV gamma rays from GRB221009A, *JCAP* **04**, 056, arXiv:2212.03477 [hep-ph].
- [68] S. Balaji, M. E. Ramirez-Quezada, J. Silk, and Y. Zhang, Light scalar explanation for the 18 TeV GRB 221009A, *Phys. Rev. D* **107**, 083038 (2023), arXiv:2301.02258 [hep-ph].
- [69] S.-Y. Guo, M. Khlopov, L. Wu, and B. Zhu, Can sterile neutrinos explain the very high energy photons from GRB221009A?, *Phys. Rev. D* **108**, L021302 (2023), arXiv:2301.03523 [hep-ph].
- [70] M. Dhuria, GRB221009A gamma-ray events from non-standard neutrino self-interactions, *Phys. Rev. D* **109**, 063007 (2024), arXiv:2309.12264 [hep-ph].
- [71] L.-Q. Gao, X.-J. Bi, J. Li, R.-M. Yao, and P.-F. Yin, Constraints on axion-like particles from the observation of GRB 221009A by LHAASO, *JCAP* **01**, 026, arXiv:2310.11391 [astro-ph.HE].
- [72] T. Piran and D. D. Ofengeim, Lorentz invariance violation limits from GRB 221009A, *Phys. Rev. D* **109**, L081501 (2024), arXiv:2308.03031 [astro-ph.HE].
- [73] Y.-M. Yang, X.-J. Bi, and P.-F. Yin, Constraints on Lorentz invariance violation from the LHAASO observation of GRB 221009A, *JCAP* **04**, 060, arXiv:2312.09079 [astro-ph.HE].
- [74] D. D. Dzhappuev *et al.*, Modernization of the Carpet-2 array of the Baksan Neutrino Observatory, *Bull. Russ. Acad. Sci. Phys.* **71**, 525 (2007).
- [75] J. Szabelski (Carpet-3), Carpet-3 - a new experiment to study primary composition around the knee, *Nucl. Phys. B Proc. Suppl.* **196**, 371 (2009), arXiv:0902.0252 [astro-ph.IM].
- [76] D. D. Dzhappuev *et al.*, Search for cosmic gamma rays with the Carpet-2 extensive air shower array (2015) arXiv:1511.09397 [astro-ph.HE].
- [77] D. D. Dzhappuev *et al.* (Carpet-3), Carpet results on astrophysical gamma rays above 100 TeV, *PoS ICRC2019*, 808 (2021), arXiv:1907.10893 [astro-ph.HE].
- [78] D. D. Dzhappuev *et al.*, Search for astrophysical PeV gamma rays from point sources with Carpet-2, *EPJ Web Conf.* **207**, 03004 (2019), arXiv:1812.02663 [astro-ph.HE].
- [79] V. Romanenko, V. Petkov, and A. Lidvansky, Ultra-high energy gamma ray astronomy with the carpet air shower array at the baksan neutrino observatory, *Journal of Experimental and Theoretical Physics* **134**, 440 (2022).
- [80] M. Amenomori *et al.*, First Detection of Photons with Energy Beyond 100 TeV from an Astrophysical Source, *Phys. Rev. Lett.* **123**, 051101 (2019), arXiv:1906.05521 [astro-ph.HE].
- [81] A. U. Abeysekara *et al.* (HAWC), Multiple Galactic Sources with Emission Above 56 TeV Detected by HAWC, *Phys. Rev. Lett.* **124**, 021102 (2020), arXiv:1909.08609 [astro-ph.HE].

- [82] Z. Cao *et al.* (LHAASO), Ultrahigh-energy photons up to 1.4 petaelectronvolts from 12 γ -ray Galactic sources, *Nature* **594**, 33 (2021).
- [83] N. Fraija *et al.*, Swift J1913.1+1946/GRB 221009A: Galactic sources of > 100 TeV-photon in spatial coincidence with the 250-TeV photon-like air shower reported by Carpet-2, *The Astronomer's Telegram* **15675** (2022).
- [84] M. Amenomori *et al.* (Tibet ASgamma), First Detection of sub-PeV Diffuse Gamma Rays from the Galactic Disk: Evidence for Ubiquitous Galactic Cosmic Rays beyond PeV Energies, *Phys. Rev. Lett.* **126**, 141101 (2021), [arXiv:2104.05181 \[astro-ph.HE\]](https://arxiv.org/abs/2104.05181).
- [85] Z. Cao *et al.* (LHAASO), Measurement of Ultra-High-Energy Diffuse Gamma-Ray Emission of the Galactic Plane from 10 TeV to 1 PeV with LHAASO-KM2A, *Phys. Rev. Lett.* **131**, 151001 (2023), [arXiv:2305.05372 \[astro-ph.HE\]](https://arxiv.org/abs/2305.05372).
- [86] D. D. Dzhappuev *et al.*, Carpet-2 search for PeV gamma rays associated with IceCube high-energy neutrino events, *Pisma Zh. Eksp. Teor. Fiz.* **109**, 223 (2019), [arXiv:1812.02662 \[astro-ph.HE\]](https://arxiv.org/abs/1812.02662).
- [87] D. Heck, J. Knapp, J. N. Capdevielle, G. Schatz, and T. Thouw, *CORSIKA: A Monte Carlo code to simulate extensive air showers*, Tech. Rep. (FZKA, 1998).
- [88] S. Ostapchenko, Monte Carlo treatment of hadronic interactions in enhanced Pomeron scheme: I. QGSJET-II model, *Phys. Rev. D* **83**, 014018 (2011), [arXiv:1010.1869 \[hep-ph\]](https://arxiv.org/abs/1010.1869).
- [89] G. Battistoni, S. Muraro, P. R. Sala, F. Cerutti, A. Ferrari, S. Roesler, A. Fassio, and J. Ranft, The FLUKA code: Description and benchmarking, *AIP Conf. Proc.* **896**, 31 (2007).
- [90] R. Conceição, L. Gibilisco, M. Pimenta, and B. Tomé, Gamma/hadron discrimination at high energies through the azimuthal fluctuations of air shower particle distributions at the ground, *JCAP* **10**, 086, [arXiv:2204.12337 \[hep-ph\]](https://arxiv.org/abs/2204.12337).
- [91] S. Navas *et al.* (Particle Data Group), Review of particle physics, *Phys. Rev. D* **110**, 030001 (2024).
- [92] H. Ayala and HAWC Collaboration, GRB 221009A: Upper limits from HAWC 8 hours after trigger, GRB Coordinates Network **32683**, 1 (2022).
- [93] Z.-Q. Xia, Y. Wang, Q. Yuan, and Y.-Z. Fan, A delayed 400 GeV photon from GRB 221009A and implication on the intergalactic magnetic field, *Nature Commun.* **15**, 4280 (2024), [arXiv:2210.13052 \[astro-ph.HE\]](https://arxiv.org/abs/2210.13052).
- [94] B. Stern and I. Tkachev, GRB 221009A, Its Precursor, and Two Afterglows in the Fermi Data, *JETP Lett.* **118**, 553 (2023), [arXiv:2303.03855 \[astro-ph.HE\]](https://arxiv.org/abs/2303.03855).
- [95] M. Axelsson *et al.* (Fermi-LAT, Fermi-GBM), GRB 221009A: the B.O.A.T Burst that Shines in Gamma Rays, (2024), [arXiv:2409.04580 \[astro-ph.HE\]](https://arxiv.org/abs/2409.04580).
- [96] H. Abdalla *et al.* (H.E.S.S.), Revealing x-ray and gamma ray temporal and spectral similarities in the GRB 190829A afterglow, *Science* **372**, 1081 (2021), [arXiv:2106.02510 \[astro-ph.HE\]](https://arxiv.org/abs/2106.02510).
- [97] E. Derishev and T. Piran, The physical conditions of the afterglow implied by magic's sub-teV observations of grb 190114c, *The Astrophysical Journal Letters* **880**, L27 (2019).
- [98] P. Kumar, R. A. Hernandez, Z. Bosnjak, and R. B. Duran, Maximum synchrotron frequency for shock-accelerated particles, *Mon. Not. Roy. Astron. Soc.* **427**, L40 (2012), [arXiv:1210.6033 \[astro-ph.HE\]](https://arxiv.org/abs/1210.6033).
- [99] T. A. Dzhatdov, E. V. Khalikov, V. S. Latypova, E. I. Podlesnyi, and I. A. Vaiman, Modelling the persistent low-state γ -ray emission of the PKS 1510–089 blazar with electromagnetic cascades initiated in hadronuclear interactions, *Mon. Not. Roy. Astron. Soc.* **515**, 5242 (2022), [arXiv:2111.07389 \[astro-ph.HE\]](https://arxiv.org/abs/2111.07389).
- [100] T. A. Dzhatdov, Probing the near and far environments of the brightest of all time grb 221009a with gamma-rays, Talk at the RICAP-24 conference (2024).
- [101] V. S. Berezhinskii and O. F. Prilutskii, A mechanism for the escape of cosmic rays from dense supernova envelopes, *Soviet Astronomy Letters* **3**, 141 (1977).
- [102] D. Eichler and P. J. Wiita, Neutron beams in active galactic nuclei, *Nature* **274**, 38–39 (1978).
- [103] J. G. Kirk and A. Mastichiadis, Neutrons from active galactic nuclei, *Astron. Astrophys.* **213**, 75 (1989).
- [104] W. Tkaczyk, Energy transport by relativistic neutrons from the core of active galactic nuclei, *The Astrophysical Journal Supplement Series* **92**, 611 (1994).
- [105] A. M. Atoyan and C. D. Dermer, Neutral beams from blazar jets, *The Astrophysical Journal* **586**, 79–96 (2003).
- [106] C. D. Dermer and A. Atoyan, Neutral beam model for the anomalous gamma-ray emission component in GRB 941017, *Astron. Astrophys.* **418**, L5 (2004), [arXiv:astro-ph/0401115](https://arxiv.org/abs/astro-ph/0401115).
- [107] R. Abbasi *et al.* (IceCube), Limits on Neutrino Emission from GRB 221009A from MeV to PeV Using the IceCube Neutrino Observatory, *Astrophys. J. Lett.* **946**, L26 (2023), [Erratum: *Astrophys.J.Lett.* 970, L43 (2024), Erratum: *Astrophys.J.* 970, L43 (2024)], [arXiv:2302.05459 \[astro-ph.HE\]](https://arxiv.org/abs/2302.05459).
- [108] S. Aiello *et al.* (KM3NeT), Search for neutrino emission from GRB 221009A using the KM3NeT ARCA and ORCA detectors, *JCAP* **08**, 006, [arXiv:2404.05354 \[astro-ph.HE\]](https://arxiv.org/abs/2404.05354).
- [109] A. Saldana-Lopez, A. Domínguez, P. G. Pérez-González, J. Finke, M. Ajello, J. R. Primack, V. S. Paliya, and A. Desai, An observational determination of the evolving extragalactic background light from the multiwavelength HST/CANDELS survey in the Fermi and CTA era, *Mon. Not. Roy. Astron. Soc.* **507**, 5144 (2021), [arXiv:2012.03035 \[astro-ph.CO\]](https://arxiv.org/abs/2012.03035).
- [110] F. Chollet *et al.*, Keras, <https://keras.io> (2015).
- [111] M. Abadi *et al.*, TensorFlow: Large-scale machine learning on heterogeneous systems, software available from tensorflow.org.